



Citation for published version:

Barbieri, E, Cammarano, A, De Rosa, S & Franco, F 2009, 'Waveguides of a Composite Plate by using the Spectral Finite Element Approach', *Journal of Vibration and Control*, vol. 15, no. 3, pp. 347-367.
<https://doi.org/10.1177/1077546307087455>

DOI:

[10.1177/1077546307087455](https://doi.org/10.1177/1077546307087455)

Publication date:

2009

[Link to publication](#)

University of Bath

General rights

Copyright and moral rights for the publications made accessible in the public portal are retained by the authors and/or other copyright owners and it is a condition of accessing publications that users recognise and abide by the legal requirements associated with these rights.

Take down policy

If you believe that this document breaches copyright please contact us providing details, and we will remove access to the work immediately and investigate your claim.

Waveguides of a Composite Plate by using the Spectral Finite Element Approach

E. BARBIERI

*Department of Mechanical Engineering, University of Bath, Bath BA2 7AY, UK
(e.barbieri@bath.ac.uk)*

A. CAMMARANO

S. DE ROSA

F. FRANCO

elab - Vibration and Acoustics Laboratory, Dipartimento di Ingegneria Aerospaziale, Università degli Studi di Napoli Federico II, 80125 Via Claudio, Napoli, Italy

Received 15 May 2007; accepted 15 October 2007

Abstract: This work presents the extension of an existing procedure for evaluating the waveguides and the dispersion curves of a laminate made up of thin orthotropic composite plates arbitrarily oriented. The adopted approach is based on one-dimensional finite-element mesh throughout the thickness. Stiffness and mass matrices available in the literature for isotropic material are reported in full expanded form for the selected problem. The aim of the work is the development of a tool for the simulation of the most common composite materials. The knowledge of the wave characteristics in a plate allows correct sizing of the numerical mesh for the frequency-dependent analysis. The development of new stiffness matrices and the analysis for different heading angles are detailed to take into account the general anisotropic nature of the composite. The procedure concerns a standard polynomial eigenvalue problem in the wavenumber variable and is focused on the evaluation of the dispersion curves for all the propagating waves within the materials. A comparison with an analytical approach is also shown in the results using the classical laminate plate theory (CLPT). However, limits of CLPT are outlined and spectral finite element method can be successfully used to overcome such limitations.

Keywords: waveguides, dispersion, composite plate, wavenumber, modal density.

1. INTRODUCTION AND STATEMENT OF THE PROBLEM

The wide and increasing use of innovative materials in transportation engineering is one of the most fascinating challenges of material science. In the aerospace field, this challenge can be defined as always being open since manufacturers are continuously looking for stiffer, robust, long-life and lighter structural components. The need for such material performance has driven for a long time the focus on fiber-reinforced composite materials and now they are a standard in several fields of transportation engineering design. One of the main problems of these innovative materials is their vibroacoustic behavior, since sometimes

the lightness requirement is in conflict with the acoustic target. Hence, in the design phase there is the need to simulate the dynamic behavior of innovative materials. This target can be obtained by using deterministic methods (Cook et al., 1989) and also energy methods (Lyon, 1975). The deterministic techniques, such as finite-element analysis (FEA), work by discretizing the given wavelength. In principle, they can be used for evaluating the response at any excitation frequency, but the computational cost (CPU time) can become easily unacceptable. In the absence of any analytical development, the deterministic techniques model directly the wavelength, by assigning at least five solution points (four elements) for each complete wave (Cook et al., 1989; Cremer et al., 2005). For increasing excitation frequency, the response becomes global, that is any quadratic mean can represent the overall behavior, and the possibility to discriminate the dynamic response among different points in space is lost. The best technique working under these conditions is the well-known statistical energy analysis (SEA) (Lyon, 1975). In Ghinet et al. (2005), for example, a SEA method for the transmission loss of sandwich shells is illustrated, in which the dispersion properties of laminates are exploited. Finnveden (2004) studied the waveguides in thin-walled structures with a finite-element formulation in order to compute group velocity and modal density as input to a SEA model. Wave propagation in laminated composite plates and rods (Baz, 2000) has been treated in depth by numerous authors in the past. Datta et al. (1988) have applied a stiffness method for a laminate made of transversely isotropic laminae, while in Nayfeh (1991) dispersion curves for anisotropic laminates are analytically extracted by the means of the transfer matrix method. A similar method can be found in Wang and Yuan (2007) for the evaluation of the group velocities and their applications in non-destructive techniques. Chitnis et al. (2001) used a higher-order theory displacement based formulation. In-plane elastic waves in a composite panel are investigated in Žak et al. (2006) with a spectral finite-element approach in the time domain. Birgersson et al. (2004) also used a spectral approach for modelling turbulence-induced vibration in pipes. In FEA, the knowledge of the wavelength is absolutely mandatory for proceeding with the mesh sizing and for selecting the proper elements; in SEA, detailed information about the group velocity and the modal density are necessary for the characterization of the specific subsystem and for later moving to analyze the energy exchange through a wave approach. The wavenumber function versus the excitation frequency (dispersion curves) for each structural wave contains the subsystem properties. Shorter (2004) and Mace et al. (2005) stressed this point with great attention. Shorter (2004) proposed an efficient approach for simulating an infinite flat plate, in which a low-cost one-dimensional finite element was used for simulating the propagating waves inside the materials. Furthermore, Mace et al. (2005) proposed the direct use of a finite-element model assembled to evaluate the modal response to obtain the dispersion curves. Two-dimensional approaches are also present in the literature (Johnson and Kienholz, 1982) and the work by Heron (2002) has to be considered as one of the first addressing the problem of the dynamic response of a generic laminate. An extensive analysis of the related literature is reported in Shorter (2004). Nevertheless, it is worth mentioning the applications of spectral finite elements in wave propagation for laminates, see for example Roy Mahapatra and Gopalakrishnan (2003), Mahapatra et al. (2006) and Chakraborty and Gopalakrishnan (2006) in the frequency domain, whereas a time-domain-based spectral element with high-order shape functions are used in Kudela et al. (2007). The present work is a straight extension of the approach proposed by Shorter (2004). A one-dimensional finite-element model is developed for a generic plate made by a laminate composite. The

approach in Shorter (2004) assumes an isotropic stress–strain relationship through the use of two independent variables for each material.

In the present work the proper stiffness and mass matrices are developed for each lamina introducing a local reference system, and the whole laminate is assembled in a global reference system. At that point a spectral finite element approach (SFEA) is used (Shorter, 2004; Mace et al., 2005). The *spectral* term refers to the fact that the method is based on the wavenumber at a given excitation frequency rather than the classical analysis of natural frequencies. The SFEA used here is the same as that presented in Shorter (2004): a full 3D displacement field within the laminate with 1D elements. In the present development, a 3D orthotropic stress–strain relationship is used (Jones, 1999), together with the proper transformation from the local reference system (lamina) to the global one (laminate). The problem for a homogeneous, isotropic plate is given in Section 2. While the dispersion properties of a homogeneous plate are independent of the heading angle ϕ , for a generic composite plate this is not true because of its anisotropic nature. Indeed, in a 2D orthotropic material, for example, the principal directions of elasticity being x and y , with $E_x \neq E_y$, the wavenumber at a fixed frequency changes with the angle from x to y according to an elliptic pattern. Then if an isotropic plate is considered that pattern is circular. In Section 3 an analytic formulation for a thin composite plate is derived, following the assumptions of the classical laminate plate theory (CLPT) (Jones, 1999). A displacements 3D free wave is then imposed on the thin plate leading to a polynomial eigenvalue problem in k where k is the wavenumber. Bending, shear and longitudinal waves can be easily identified from the resulting equations. Furthermore, a spectral finite-element method (SFEM) will be used to obtain the dispersion curves for a generic composite plate and then compared to the analytical approach. These results are shown in Section 6 in the form of polar patterns at fixed frequency and spectra at fixed heading angle. Section 4 is devoted to the overall development of the required SFEM matrices. Section 5 is centered on the solution of the characteristic equation, and the results are presented in Section 6. These results are for both a homogeneous and a composite plate. The work is concluded in Section 7 where some considerations are given about the validity of the CLPT. It is demonstrated how the present numerical method can work with any configuration, overcoming the limitations of the standard theoretical models.

2. THE HOMOGENEOUS PLATE

A uniform thin and flat plate is considered, made of a homogeneous material. From classical thin plate theory (Leissa, 1993) it is well known that three waves will propagate in the material of thickness h : longitudinal, shear and bending waves. Each of these is associated with the respective wavenumber k_l , k_s and k_b :

$$k_l^2 = \frac{(1 - \nu^2)\rho}{E}\omega^2, \quad k_s^2 = \frac{2(1 + \nu)\rho}{E}\omega^2, \quad k_b^4 = \frac{12(1 - \nu^2)\rho}{Eh^2}\omega^2. \quad (1)$$

In Equation (1) the longitudinal wave speed $C_l(\omega)^2 = \frac{E}{\rho(1-\nu^2)}$, the shear wave speed $C_s(\omega)^2 = \frac{E}{2\rho(1+\nu)}$ and the plate bending stiffness $D = \frac{Eh^2}{12\rho(1-\nu^2)}$. The generic group velocity and the wavelength for each wave can be defined by using the definition

$$C_g = \frac{\partial \omega}{\partial k_g}, \quad \lambda = \frac{C_g}{f} \quad (2)$$

and the modal density for a plate of area A (Lyon, 1975)

$$n_g(\omega) = \frac{A}{2\pi^2} \frac{k(\omega)}{c_g(\omega)}. \quad (3)$$

By using these relationships, any information for a predictive methodology, deterministic or energetic, can be obtained. In fact, the mesh of the predictive finite-element model could be designed to work up to a given excitation frequency. The model will be completed with the specific boundary conditions. For the energy methods all is known about the plate, for a given material and dimensions. Both the predictive models have to be completed including the damping information. In the following sections, a SFEM will be used to find the dispersion curves for a generic composite plate and the results will be compared to those obtained from the analytical approach.

3. ANALYTICAL STRUCTURAL WAVEGUIDES FOR A THIN COMPOSITE PLATE

According to the assumptions of the classical thin plate theory, in a plane stress problem the following equations of equilibrium can be written (Timoshenko and Goodier, 1970):

$$\frac{\partial N_x}{\partial x} + \frac{\partial N_{xy}}{\partial y} - \rho_s \ddot{u} = 0, \quad (4)$$

$$\frac{\partial N_{xy}}{\partial x} + \frac{\partial N_y}{\partial y} - \rho_s \ddot{v} = 0, \quad (5)$$

$$\frac{\partial^2 M_x}{\partial x^2} + \frac{\partial^2 M_y}{\partial y^2} + 2 \frac{\partial^2 M_{xy}}{\partial x \partial y} - \rho_s \ddot{w} = 0, \quad (6)$$

where N_x , N_y and N_{xy} are shearing forces per unit length, M_x , M_y are the bending moments per unit length and M_{xy} the twisting moments per unit length, while ρ_s is the surface mass density. For a composite plate, the following relationships between force, moment and strain curvatures can be established (Jones, 1999):

$$\mathbf{N} = \mathbf{A}\epsilon^0 + \mathbf{B}\kappa, \quad (7)$$

$$\mathbf{M} = \mathbf{B}\epsilon^0 + \mathbf{D}\kappa, \quad (8)$$

where ϵ^0 are the strains of the middle plane,

$$\boldsymbol{\epsilon}^0 = \begin{bmatrix} \epsilon_x \\ \epsilon_y \\ \epsilon_{xy} \end{bmatrix} = \begin{bmatrix} \frac{\partial u}{\partial x} \\ \frac{\partial v}{\partial y} \\ \frac{\partial u}{\partial y} + \frac{\partial v}{\partial x} \end{bmatrix} \quad (9)$$

and κ are the curvatures of the middle plane,

$$\boldsymbol{\kappa} = \begin{bmatrix} \kappa_x \\ \kappa_y \\ \kappa_{xy} \end{bmatrix} = \begin{bmatrix} -\frac{\partial^2 w}{\partial x^2} \\ -\frac{\partial^2 w}{\partial y^2} \\ -2\frac{\partial^2 w}{\partial x \partial y} \end{bmatrix}. \quad (10)$$

The following 3D displacement wave is assumed to propagate along the plate:

$$\begin{bmatrix} u(x, y, t) \\ v(x, y, t) \\ w(x, y, t) \end{bmatrix} = \begin{bmatrix} U \\ V \\ W \end{bmatrix} e^{j[k(\cos(\phi)x + \sin(\phi)y) - \omega t]}, \quad (11)$$

where ϕ is the heading angle of the wave, u , v and w are respectively the displacement fields in the x , y and z axes, and U , V and W are the respective magnitudes of the propagating wave. Substituting Equations (7)–(10) into (4)–(6) and with the assumed displacement field (11), the following polynomial eigenproblem in k is obtained:

$$\begin{bmatrix} -k^2 \mathbf{L}^T \mathbf{A} \mathbf{L}, & jk^3 \mathbf{L}^T \mathbf{B} \mathbf{P} \\ -jk^3 \mathbf{P}^T \mathbf{B} \mathbf{L}, & -k^4 \mathbf{P}^T \mathbf{D} \mathbf{P} \end{bmatrix} \begin{bmatrix} U \\ V \\ W \end{bmatrix} + \rho_s \omega^2 \mathbf{I} \begin{bmatrix} U \\ V \\ W \end{bmatrix} = 0, \quad (12)$$

where

$$\mathbf{L} = \begin{bmatrix} \cos(\phi) & 0 \\ 0 & \sin(\phi) \\ \sin(\phi) & \cos(\phi) \end{bmatrix}, \quad (13)$$

$$\mathbf{P}^T = \begin{bmatrix} \cos^2(\phi) & \sin^2(\phi) & 2 \sin(\phi) \cos(\phi) \end{bmatrix}. \quad (14)$$

If a symmetric laminate is considered, then $\mathbf{B} = 0$ and the polynomial problem (12) can be de-coupled into the following two eigenproblems:

$$-k^2 \mathbf{L}^T \mathbf{A} \mathbf{L} \begin{bmatrix} U \\ V \end{bmatrix} + \rho_s \omega^2 \mathbf{I} \begin{bmatrix} U \\ V \end{bmatrix} = 0, \quad (15)$$

$$-k^4 \mathbf{P}^T \mathbf{D} \mathbf{P} W + \rho_s \omega^2 W = 0. \quad (16)$$

It can be seen from Equation (15) that, being coupled shear-longitudinal waves, $k \propto \omega$ while from Equation(16) for the flexural wave it follows that $k \propto \sqrt{\omega}$. Indeed, from Equation (16) it can be directly derived that the flexural wavenumber is

$$k_f(\phi, \omega) = \sqrt[4]{\frac{\rho_s}{\mathbf{P}^T \mathbf{D} \mathbf{P}}} \sqrt{\omega}. \quad (17)$$

For Equation (15), if ξ_l and ξ_s are the two eigenvalues of the matrix $\mathbf{L}^T \mathbf{A} \mathbf{L}$, then

$$k_s(\phi, \omega) = \sqrt{\frac{\rho_s}{\xi_s(\phi)}} \omega, \quad k_e(\phi, \omega) = \sqrt{\frac{\rho_s}{\xi_e(\phi)}} \omega. \quad (18)$$

Using Equation (2), the group velocities can easily be evaluated:

$$C_f = 2 \sqrt[4]{\frac{\mathbf{P}^T \mathbf{D} \mathbf{P}}{\rho_s}} \sqrt{\omega}, \quad C_s = \sqrt{\frac{\xi_s(\phi)}{\rho_s}}, \quad C_e = \sqrt{\frac{\xi_e(\phi)}{\rho_s}}. \quad (19)$$

4. ASSEMBLY OF MATRICES

4.1. Variational Formulation

With the intent of establishing a finite-element model, Hamilton's principle is used,

$$\delta \left[\int (T + U) dt \right] = 0, \quad (20)$$

where T is the kinetic energy and U is the strain energy. If a time average over a period is considered, then

$$\bar{T} = \frac{1}{2} \int_{\Omega} \dot{\mathbf{d}}^H \rho \dot{\mathbf{d}} \, d\Omega, \quad (21)$$

where \mathbf{d} is the displacements field, ρ is the mass density and the superscript H means hermitian,

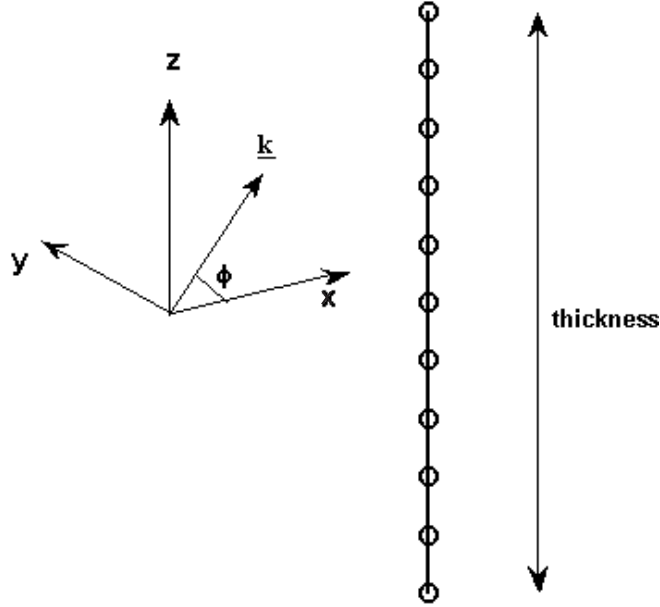


Figure 1. 1D mesh.

$$\bar{U} = \frac{1}{2} \int_{\Omega} \mathbf{e}^H \mathbf{s} \, d\Omega = \frac{1}{2} \int_{\Omega} \mathbf{e}^H \mathbf{C}_{x-y} \mathbf{e} \, d\Omega, \quad (22)$$

where \mathbf{e} is the vectorized strain tensor and \mathbf{s} is the vectorized stress tensor in the laminate reference system, \mathbf{C}_{x-y} is the stress-strain relationship matrix in the laminate reference and Ω is the space domain made of a single element of length L and an arbitrary rectangular domain in the plane x - y .

4.2. Finite-element Displacement Fields

Assuming that x is the direction of the propagating wave (Figure 1) with frequency ω , the wavenumber is k and the heading angle is ϕ , the displacement field can be approximated as

$$\mathbf{d}(x, y, z, t) = \begin{bmatrix} u(z) \\ v(z) \\ w(z) \end{bmatrix} e^{j[\omega t - k(\cos(\phi)x + \sin(\phi)y)]}. \quad (23)$$

Equation (23) resembles Equation (11), with the only exception being that in Equation (11) the displacements refer to a plane stress problem, while in Equation (23) a full 3D stress-strain problem is considered. The displacements at $x = 0$ for the single element of length L can be approximated by the following one-dimensional interpolating function:

$$\begin{bmatrix} u(z) \\ v(z) \\ w(z) \end{bmatrix} = \begin{bmatrix} \mathbf{N}_i(z) & 0 & 0 \\ 0 & \mathbf{N}_i(z) & 0 \\ 0 & 0 & \mathbf{N}_i(z) \end{bmatrix} \begin{bmatrix} \mathbf{q}_u \\ \mathbf{q}_v \\ \mathbf{q}_w \end{bmatrix} = \mathbf{N}(z) \cdot \mathbf{q}_0, \quad (24)$$

with $\mathbf{N}(z)$ the matrix of shape functions (size 3×6) and \mathbf{q}_0 the vector of complex amplitudes of nodal displacements (Cook et al., 1989)

$$\mathbf{N}_i(z) = \begin{bmatrix} 1 - \frac{z}{L} & \frac{z}{L} \end{bmatrix}, \quad (25)$$

$$\begin{bmatrix} \mathbf{q}_u \\ \mathbf{q}_v \\ \mathbf{q}_w \end{bmatrix} = \begin{bmatrix} u_1 \\ u_2 \\ v_1 \\ v_2 \\ w_1 \\ w_2 \end{bmatrix}. \quad (26)$$

4.3. Definition of Stiffness and Mass Matrices

The strain in the element is

$$\mathbf{e}(x, y, z, t) = \begin{bmatrix} \epsilon_{xx} \\ \epsilon_{yy} \\ \epsilon_{zz} \\ \gamma_{yz} \\ \gamma_{xz} \\ \gamma_{xy} \end{bmatrix} = \begin{bmatrix} \frac{\partial}{\partial x} & 0 & 0 \\ 0 & \frac{\partial}{\partial y} & 0 \\ 0 & 0 & \frac{\partial}{\partial z} \\ \frac{\partial}{\partial y} & \frac{\partial}{\partial x} & 0 \\ \frac{\partial}{\partial z} & 0 & \frac{\partial}{\partial x} \\ 0 & \frac{\partial}{\partial z} & \frac{\partial}{\partial y} \end{bmatrix} \mathbf{d}. \quad (27)$$

By using Equation (23),

$$\mathbf{e}(x, y, z, t) = \mathbf{F}(k, \phi, z) \cdot \mathbf{q}_0 e^{j[\omega t - k(\cos(\phi)x + \sin(\phi)y)]}, \quad (28)$$

where the strain-displacement matrix $\mathbf{F}(k, \phi, z)$ (size 6×6) is given by

$$\mathbf{F}(k, \phi, z) = \begin{bmatrix} -jk \cos(\phi)\mathbf{N}_i(z) & 0 & 0 \\ 0 & -jk \sin(\phi)\mathbf{N}_i(z) & 0 \\ 0 & 0 & \frac{\partial \mathbf{N}_i}{\partial z} \\ 0 & \frac{\partial \mathbf{N}_i}{\partial z} & -jk \sin(\phi)\mathbf{N}_i(z) \\ \frac{\partial \mathbf{N}_i}{\partial z} & 0 & -jk \cos(\phi)\mathbf{N}_i(z) \\ -jk \sin(\phi)\mathbf{N}_i(z) & -jk \cos(\phi)\mathbf{N}_i(z) & 0 \end{bmatrix}. \quad (29)$$

Now it is necessary to introduce a stress-strain relationship for a 3D orthotropic material in the lamina reference Ox_Ly_L . For this kind of material, nine independent engineering constants are needed (Jones, 1999):

$$\mathbf{s}_L = \mathbf{C}_L \cdot \mathbf{e}_L, \quad \mathbf{C}_L = \mathbf{S}_L^{-1}, \quad (30)$$

$$\mathbf{S}_L = \begin{bmatrix} \frac{1}{E_{11}} & \frac{-\nu_{21}}{E_{22}} & \frac{-\nu_{31}}{E_{33}} & 0 & 0 & 0 \\ \frac{-\nu_{12}}{E_{11}} & \frac{1}{E_{22}} & \frac{-\nu_{32}}{E_{33}} & 0 & 0 & 0 \\ \frac{-\nu_{13}}{E_{11}} & \frac{-\nu_{23}}{E_{22}} & \frac{1}{E_{33}} & 0 & 0 & 0 \\ 0 & 0 & 0 & \frac{1}{G_{23}} & 0 & 0 \\ 0 & 0 & 0 & 0 & \frac{1}{G_{31}} & 0 \\ 0 & 0 & 0 & 0 & 0 & \frac{1}{G_{12}} \end{bmatrix}, \quad (31)$$

where the matrix is symmetric from Betti's theorem (Jones, 1999),

$$\frac{\nu_{ij}}{E_{ii}} = \frac{\nu_{ji}}{E_{jj}}, \quad i, j = 1, 2, 3. \quad (32)$$

Then the following tensorial reference transformation between lamina reference and laminate reference Oxy is introduced (Figure 2):

$$\mathbf{C}_{x-y} = \mathbf{T}(\theta)^{-1} \mathbf{C}_L \mathbf{R} \mathbf{T}(\theta) \mathbf{R}^{-1}, \quad (33)$$

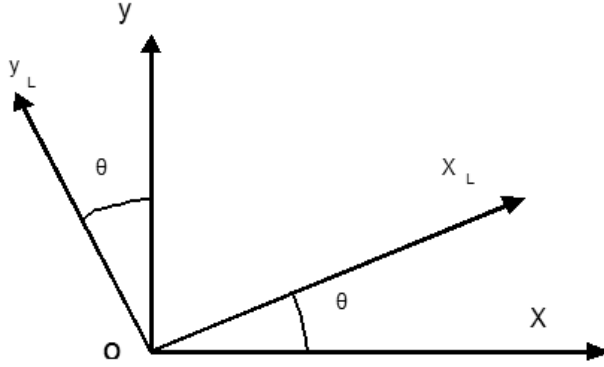


Figure 2. Reference transformation between lamina reference $O_{x_L y_L}$ and laminate reference $O_{x y}$.

where θ is the angle between the x_L - y_L axis and the x - y axis (the z -axis is the same for both references),

$$\mathbf{T}(\theta) = \begin{bmatrix} \cos^2(\theta) & \sin^2(\theta) & 0 & 0 & 0 & 2 \sin(\theta) \cos(\theta) \\ \sin^2(\theta) & \cos^2(\theta) & 0 & 0 & 0 & -2 \sin(\theta) \cos(\theta) \\ 0 & 0 & 1 & 0 & 0 & 0 \\ 0 & 0 & 0 & \cos(\theta) & -\sin(\theta) & 0 \\ 0 & 0 & 0 & \sin(\theta) & \cos(\theta) & 0 \\ -\sin(\theta) \cos(\theta) & \sin(\theta) \cos(\theta) & 0 & 0 & 0 & \cos^2(\theta) - \sin^2(\theta) \end{bmatrix}, \quad (34)$$

and

$$\mathbf{R} = \begin{bmatrix} 1 & 0 & 0 & 0 & 0 & 0 \\ 0 & 1 & 0 & 0 & 0 & 0 \\ 0 & 0 & 1 & 0 & 0 & 0 \\ 0 & 0 & 0 & 2 & 0 & 0 \\ 0 & 0 & 0 & 0 & 2 & 0 \\ 0 & 0 & 0 & 0 & 0 & 2 \end{bmatrix}. \quad (35)$$

Then the time-averaged kinetic and strain energies can be evaluated as

$$\bar{T} = -\frac{1}{2}\omega^2\mathbf{q}_0^H \left[\int_{\Omega} \mathbf{N}(z)^T \rho \mathbf{N}(z) d\Omega \right] \mathbf{q}_0, \quad (36)$$

$$\bar{U} = \frac{1}{2}\mathbf{q}_0^H \left[\int_{\Omega} \mathbf{F}(k, \phi, z)^H \mathbf{C}_{x-y} \mathbf{F}(k, \phi, z) d\Omega \right] \mathbf{q}_0. \quad (37)$$

Substituting Equations (36) and (37) into Equation (20), we have

$$\delta \left[-\frac{\omega^2}{2}\mathbf{q}_0^T \mathbf{M} \mathbf{q}_0 + \frac{1}{2}\mathbf{q}_0^T \mathbf{K}(k, \phi) \mathbf{q}_0 \right] = 0, \quad (38)$$

where the mass and stiffness matrices are defined as

$$\mathbf{M} = \int_0^L \mathbf{N}(z)^T \rho \mathbf{N}(z) dz, \quad (39)$$

and

$$\mathbf{K}(k, \phi) = \int_0^L \mathbf{F}^H(k, \phi, z) \mathbf{C}_{x-y} \mathbf{F}(k, \phi, z) dz, \quad (40)$$

where L is the length of the element. Furthermore, Equation (40) returns the case of a uniform and isotropic plate if $\theta = 0$, $E_{11} = E_{22} = E_{33} = E$, $\nu_{12} = \nu_{31} = \nu_{23} = \nu$ and $G_{12} = G_{31} = G_{23} = \frac{E}{2(1+\nu)}$. Since the strain-displacement matrix only contains terms linear in k , the stiffness matrix can be rewritten in the form

$$\mathbf{K}(k, \phi) = \mathbf{K}_2(\phi)k^2 + \mathbf{K}_1(\phi)k + \mathbf{K}_0(\phi). \quad (41)$$

A single element has six degrees of freedom. The number of eigenvalues that could be extracted from such an element is then six, which is the exact number of the propagating waves (three for both directions of travel). Moreover, even only one element can give good results for the dispersive relations in a homogeneous plate, as will be shown below. Then a rule of thumb for discretizing the thickness could be one or two elements per layer of the laminate. As the proposed mesh is a 1D discretization, all these matrices can easily be assembled in a straightforward way. Indeed, given the elastic properties of each layer, the matrices \mathbf{K}_0 , \mathbf{K}_1 , \mathbf{K}_2 and \mathbf{M} are readily calculated. Afterwards, these matrices are expanded to the size of the total number of nodes, allocated in the right position and then they are all summed in order to give the assembled matrices of the whole thickness.

5. CHARACTERISTIC EQUATION AND OUTPUT FEATURES

Using the above variational formulation, from Equation (38),

$$\delta \mathbf{q}_0^T \left[-\omega^2 \mathbf{M} \mathbf{q}_0 + \mathbf{K}(k, \phi) \mathbf{q}_0 \right] = 0 \quad \forall \delta \mathbf{q}_0, \quad (42)$$

and thus the characteristic equation takes the following form:

$$[\mathbf{K}_2(\phi)k^2 + \mathbf{K}_1(\phi)k + \mathbf{K}_0(\phi) - \omega^2\mathbf{M}]\mathbf{q}_0 = 0. \quad (43)$$

If ϕ and ω are fixed, the characteristic equation is a generalized quadratic eigenvalue problem for k and the dispersion curves result in varying frequency, while at fixed ω the polar pattern is derived when the heading angle is in the range between 0° and 360° . This kind of problem can be easily transformed into a linear one by the positions

$$\mathbf{q}_1 = k\mathbf{q}_0, \quad (44)$$

$$\mathbf{C}_2 = \mathbf{K}_2, \quad \mathbf{C}_1 = \mathbf{K}_1, \quad \mathbf{C}_0 = \mathbf{K}_0 - \omega^2\mathbf{M}, \quad (45)$$

so that

$$\begin{bmatrix} 0 & \mathbf{I} \\ -\mathbf{C}_2^{-1}\mathbf{C}_0 & -\mathbf{C}_2^{-1}\mathbf{C}_1 \end{bmatrix} \begin{bmatrix} \mathbf{q}_0 \\ \mathbf{q}_1 \end{bmatrix} - k \begin{bmatrix} \mathbf{I} & 0 \\ 0 & \mathbf{I} \end{bmatrix} \begin{bmatrix} \mathbf{q}_0 \\ \mathbf{q}_1 \end{bmatrix} = 0. \quad (46)$$

These eigenvalues can be divided in three groups:

- (i) *purely real*;
- (ii) *purely imaginary*;
- (iii) *complex*.

The eigenvalues in (i) are referred to as *propagating oscillating waves*, because from Equation (23) they generate terms with no exponential decay. The waves that exhibit an exponential decay are named *evanescent waves* and they are of two types, *non-oscillating* (eigenvalues purely imaginary) and *oscillating* (complex eigenvalues). Evanescent waves are of no interest because they do not propagate along the material, but simply extinguish with time. The sign of the real and imaginary parts of the eigenvalues indicate the direction of travel of a given wave. The eigenvectors represent the cross-sectional wave shape associated with a given wave, at a fixed frequency. It should be noted that the eigenvectors refer to a 1D domain along the z -axis.

6. RESULTS

6.1. Dispersion Curves and Eigenvector Plots

6.1.1. Homogeneous Plate

In this section the consistency with the isotropic case is shown together with a comparison with the analytical formulas (1) for an aluminium plate of thickness 0.0012 m, density 2700 kg m^{-3} , $E = 71 \times 10^9 \text{ Pa}$ and $\nu = 0.3296$.

As it can be seen from Figures (3) and (4), there is a perfect agreement with the analytical results for both spectra and polar patterns, even if only two linear elements are used; the

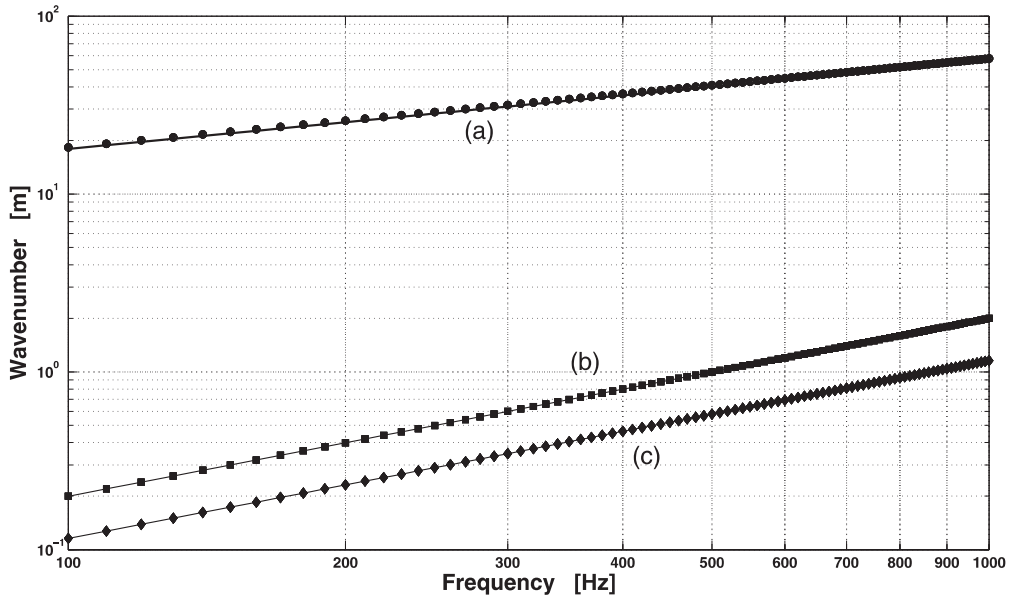


Figure 3. Homogeneous plate: continuous line, analytical results; dotted line, SFEM results. (a) Bending wave. (b) Shear wave. (c) Longitudinal wave.

Table 1. Engineering properties of the composite plate.

	Material A	Material B
E_{11}	65×10^9 Pa	145×10^9 Pa
E_{22}	65×10^9 Pa	7.79×10^9 Pa
G_{12}	3.86×10^9 Pa	4×10^9 Pa
ν_{12}	0.05	0.34
ρ	1467 kg m^{-3}	1550 kg m^{-3}
Thickness	2.37 mm	2.37 mm
Lay-up sequence	$[0A, 45B, 90B, 45B, 0B, 90B]_S$	

finite-element results also converge using simply one element. It must be pointed out that the patterns are circular, due to the isotropic nature of the material, so the dispersion curves in Figure (3) are the same for every heading angle. This is not the case for the composite plate, where a heading angle must be specified.

6.1.2. Composite Plate

The engineering properties on the plate are summarized in table 1. The transverse properties were set in order to satisfy the assumptions of plane stress on which the formulas used in Section 3 are based. One element per layer was used in the analysis.

These results agree with the analytical ones, again with spectra as in Figures (5) and patterns as in Figures (6). As can be seen from these figures, the wavenumbers are strongly dependent on the heading angle, due to the anisotropic nature of the laminate. An immediate

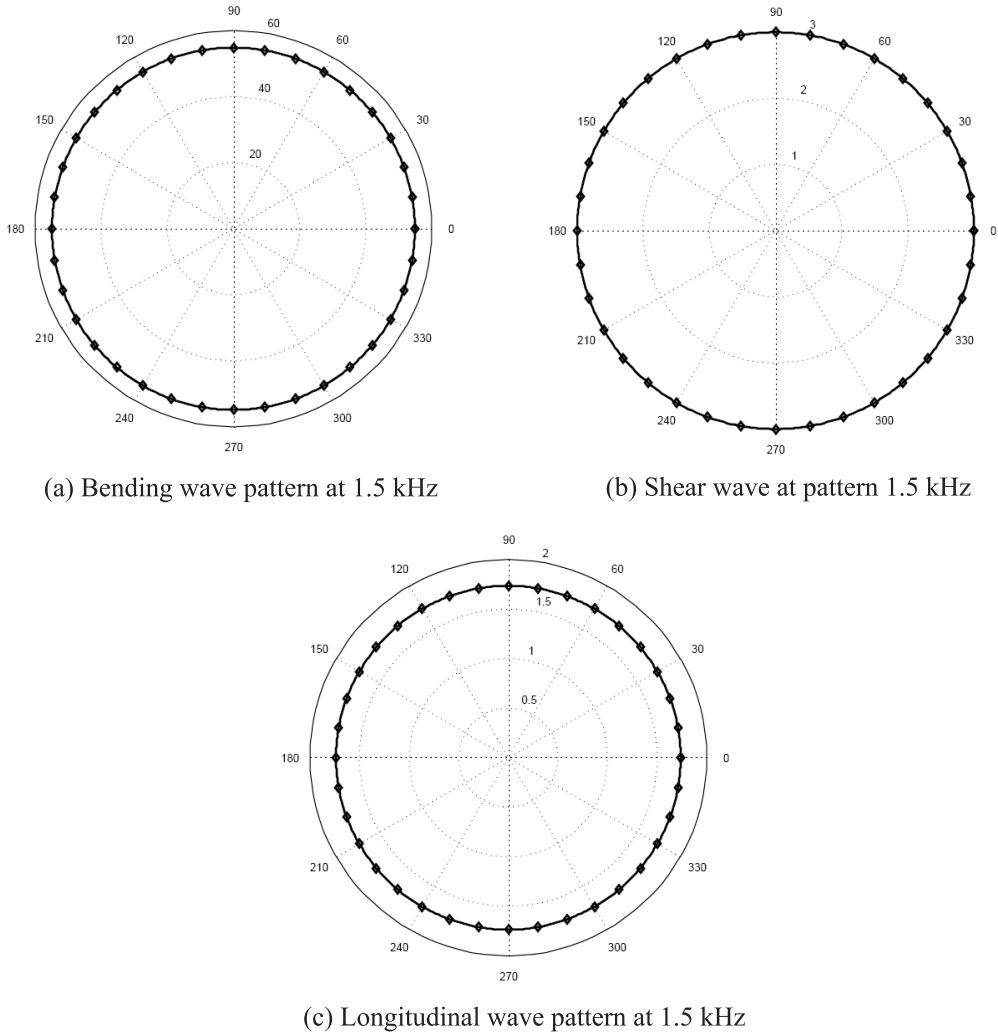
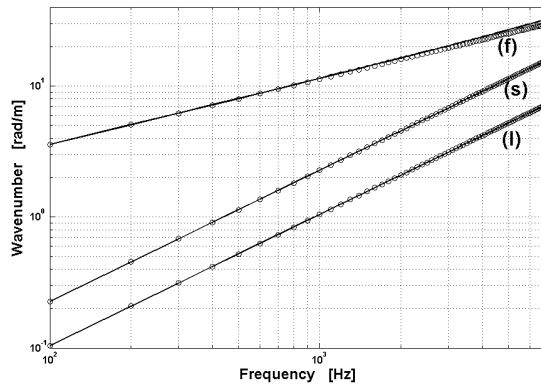
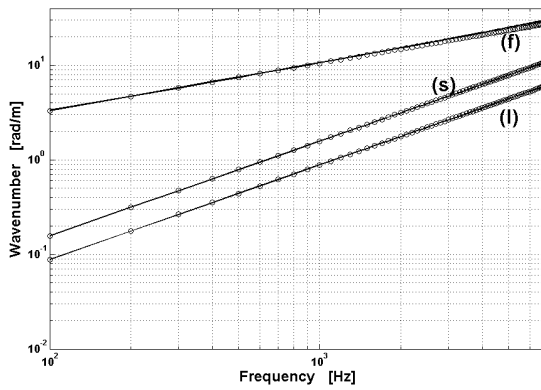


Figure 4. Polar patterns for the homogeneous plate: continuous line: analytical results; diamonds: SFEM results.

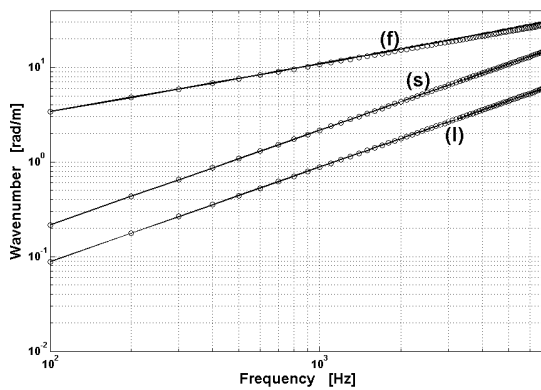
visualization of the wave as in Figures 7, (a) and (b) can be provided once the eigenvector q_0 is obtained. Then, the displacement field can be obtained from Equation (23) and then plotted over a 3D domain in the x , y and z axes. Since the domain is finite only in the z direction, the x and y limits of the domain can be chosen arbitrarily. The wave depicted in Figure 7 is a bending wave, whereas that depicted in Figure 7(b) is a shear wave and in Figure 7(c) a longitudinal wave is shown. Using Equation (2) the group velocity can be evaluated from the dispersion curves. Furthermore, when area A of the rectangular flat plate is specified, from Equation (3) the modal density curves for the propagating waves can be computed. According to a SEA formulation, these modal densities need to be averaged over the heading angle (Ghinet et al., 2005). Moreover, following (Shorter, 2004) it is also



(a) Dispersion curves at $\phi = 0^\circ$

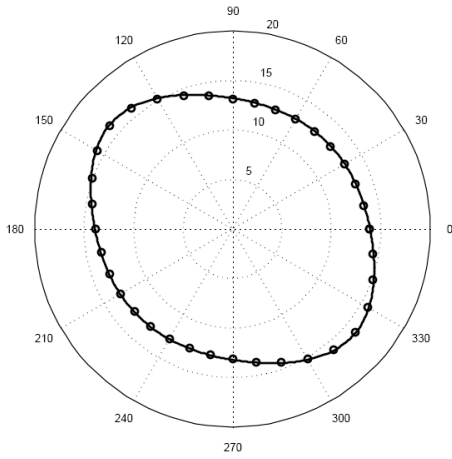


(b) Dispersion curves at $\phi = 45^\circ$

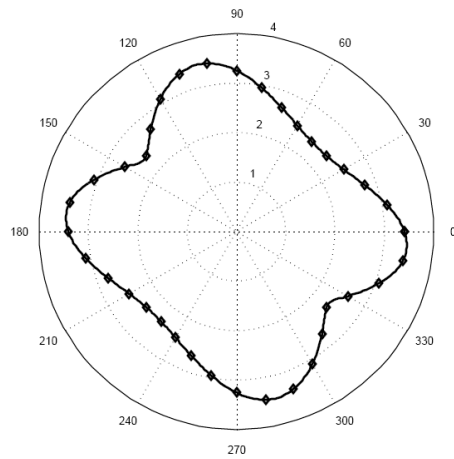


(c) Dispersion curves at $\phi = 90^\circ$

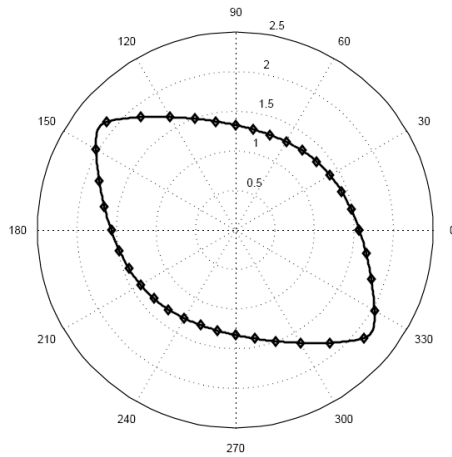
Figure 5. Dispersion curves for the composite plate: continuous line, analytical results; symbols, SFEM results. (f) flexural, (s) shear, (l) longitudinal.



(a) Bending wave pattern at 1.5 kHz



(b) Shear wave at pattern 1.5 kHz



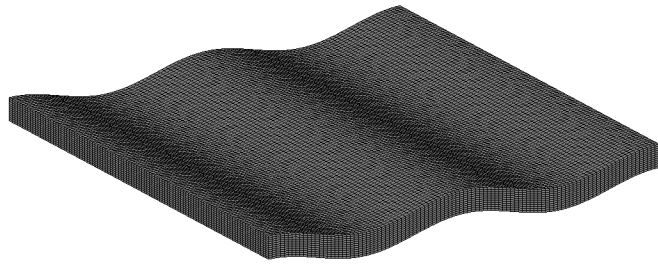
(c) Longitudinal wave pattern at 1.5 kHz

Figure 6. Polar patterns for the composite plate: continuous line, analytical results; diamonds: SFEM results.

possible to evaluate the structural damping loss factor (DLF) when a DLF for each lamina is specified. However, these details are not given here.

7. LIMITS OF CLASSICAL LAMINATE PLATE THEORY

In this section the limits of the CLPT are illustrated. For this purpose, a characteristic adimensional number could be introduced,



(a) Bending wave at 4 kHz



(b) Shear wave at 4 kHz



(c) Longitudinal wave at 4 kHz

Figure 7. Eigenvector plots for the composite plate at $\phi = 0^\circ$. Axis scales are equal, with the thickness much smaller than the wavelength.

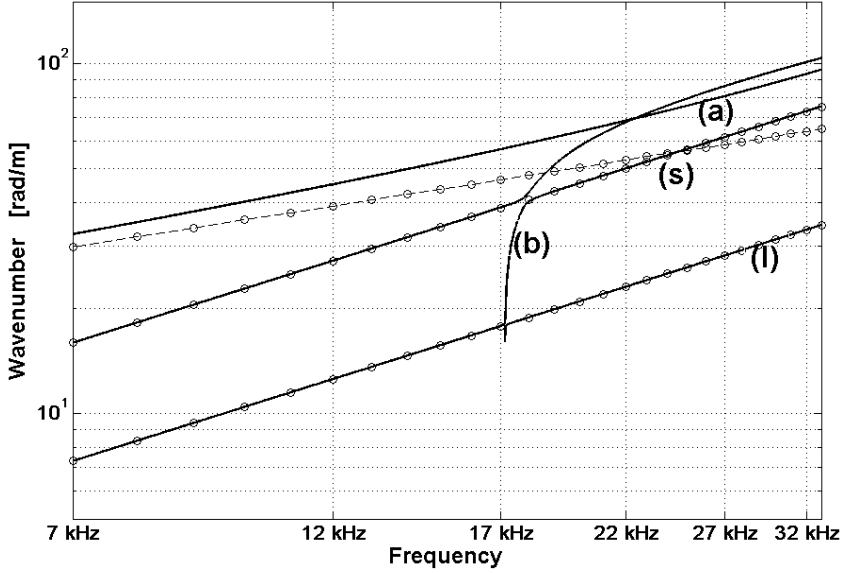


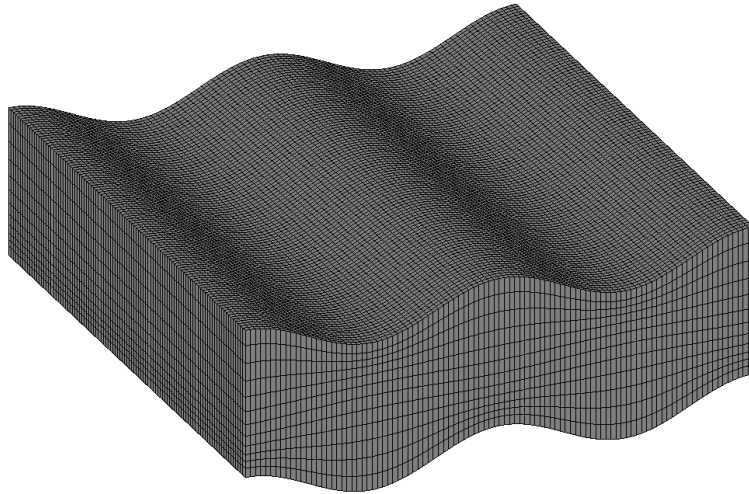
Figure 8. Dispersion curves for the composite plate: continuous Line, SFEM results; dash-dotted line, analytical results. (s) shear, (l) longitudinal, (a) and (b) new waveforms.

$$\mu = \frac{h}{\lambda}, \quad (47)$$

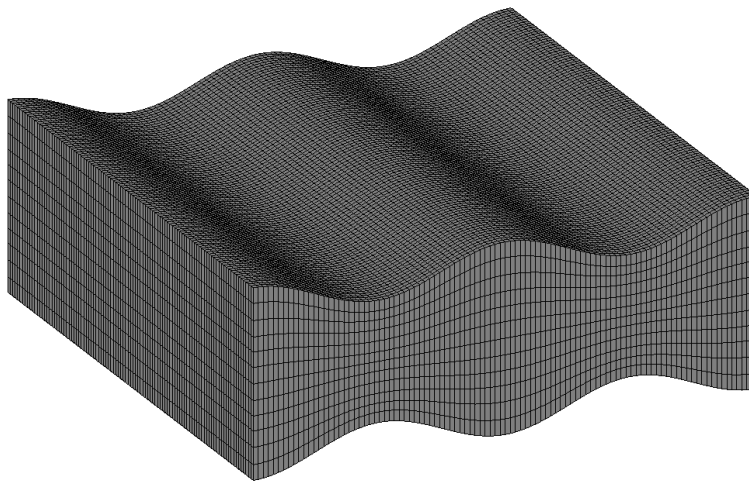
where h is the thickness of the plate and λ is the smallest wavelength (usually the flexural one). When $\mu \ll 1$ the plate could be considered thin, since h is much smaller than the characteristic length of the problem, which is the wavelength of the propagating wave. Since λ decreases with increase in frequency, at *relatively* high frequencies the analytical approach explained in Section 3 is inadequate to predict the dispersion properties of the laminate plate, because the smallest wavelength is the same order of magnitude as the thickness. The plate indeed becomes thick. The frequency limit when such an event occurs, ω_{lim} , is when $\mu \approx 1$,

$$k(\omega_{lim}) = \frac{2\pi}{h}. \quad (48)$$

New waveforms appear when $\omega \ll \omega_{lim}$ as can be seen from the dispersion plot in Figure 7 and from Figures 9. The bending wave in Figure 9(a) is slightly different from that in Figure 7 and its dispersion curve differs from the analytical theory. The wave 9(b) cannot be predicted from the CLPT since, according to the eigenproblem (12), only six eigenvalues (three for both directions of travel) are obtainable, whereas eight eigenvalues come from the SFEM above 17 kHz. Thus, when the frequency increases, a SFEM approach is useful to overcome the limits of the CLPT.



(a)



(b)

Figure 9. Eigenvector plots for the composite plate at $\phi = 0^\circ$: new waveforms at 27 kHz. Axis scales are equal, with the thickness comparable with the wavelength.

8. CONCLUSIONS

An extension to anisotropic laminates of an existing FEA-based waveguide procedure was illustrated. The laminate is made up of orthotropic layers arbitrarily oriented. Using Hamilton's variational principle, mass and stiffness matrices were developed. The followed approach is based on a 1D finite-element discretization throughout the thickness, so that a full 3D stress-strain relationship is required. An orthotropic constitutive relation is used so nine

independent variables are needed. A reference transformation between lamina and laminate was also necessary in order to introduce the lamina orientation. The resulting equation is expressed in terms of a quadratic eigenproblem in the wavenumber variable at a fixed frequency and heading angle. This problem was transformed into a linear problem and easily solved with standard numerical routines. Dispersion curves and polar patterns are obtained for the case of a uniform isotropic plate and for a laminate composite plate. Comparison with analytical formulas available from the CLPT showed good agreement with the finite-element results. Nevertheless, the analytical theory fails with increase in frequency. In fact, CLPT cannot predict the appearance of new waveforms, whereas the SFEM can identify new structural waveguides. Thus the SFEM can overcome the limits of the CLPT, allowing a more satisfactory analysis of the dispersion properties at higher frequencies. The procedure can be easily completed by including the evaluation of the resulting loss factor, given the individual loss factor of each lamina and the group velocity curves of the propagating waves, as well as their modal densities. All the present evaluations and results have been obtained by using Matlab: the m-files can be requested from the first author.

REFERENCES

- Baz, A., 2000, "Spectral finite-element modeling of the longitudinal wave propagation in rods treated with active constrained layer damping," *Smart Materials and Structures* **9**, 372–377.
- Birgersson, F., Finnveden, S., and Robert, G., 2004, "Modelling turbulence-induced vibration of pipes with a spectral finite element method," *Journal of Sound and Vibration* **278**(4–5), 749–772.
- Chakraborty, A. and Gopalakrishnan, S., 2006, "A spectral finite element model for wave propagation analysis in laminated composite plate," *Journal of Vibration and Acoustics* **128**, 477.
- Chitnis, M., Desai, Y., and Kant, T., 2001, "Wave propagation in laminated composite plates using higher order theory," *Journal of Applied Mechanics* **68**(3), 503–505.
- Cook, R., Malkus, D., Plesha, M., and Witt, R., 1989, *Concepts and Applications of Finite Element Analysis*, Wiley, New York.
- Cremer, L., Petersson, B., and Heckl, M., 2005, *Structure-Borne Sound: Structural Vibrations and Sound Radiation at Audio Frequencies*, Springer, Berlin.
- Datta, S., Shah, A., Bratton, R., and Chakraborty, T., 1988, "Wave propagation in laminated composite plates," *The Journal of the Acoustical Society of America* **83**, 2020.
- Finnveden, S., 2004, "Evaluation of modal density and group velocity by a finite element method," *Journal of Sound and Vibration* **273**(1), 51–75.
- Ghinet, S., Atalla, N., and Osman, H., 2005, "The transmission loss of curved laminates and sandwich composite panels," *The Journal of the Acoustical Society of America* **118**, 774.
- Heron, K., 2002, "Predictive SEA and anisotropic panels," in *Proceedings of the ISMA International Conference on Sound and Vibration*, Leuven, Belgium, September.
- Johnson, C. and Kienholz, D., 1982, "Finite element prediction of damping in structures with constrained viscoelastic layers," *AIAA Journal* **20**(9), 1284–1290.
- Jones, R., 1999, *Mechanics of Composite Materials*, Taylor & Francis, Philadelphia.
- Kudela, P., Žák, A., Krawczuk, M., and Ostachowicz, W., 2007, "Modelling of wave propagation in composite plates using the time domain spectral element method," *Journal of Sound and Vibration* **302**(4–5), 728–745.
- Wang, L. and Yuan, F. G., 2007, "Group velocity and characteristic wave curves of Lamb waves in composites: Modeling and experiments," *Composites Science and Technology* **67**, 1370–1384.
- Leissa, A., 1993, *Vibration of Plates*, Published for the Acoustical Society of America through the American Institute of Physics, New York.
- Lyon, R., 1975, *Statistical Energy Analysis of Dynamical Systems: Theory and Applications*, MIT Press, Cambridge, MA.
- Mace, B., Duhamel, D., Brennan, M., and Hinke, L., 2005, "Finite element prediction of wave motion in structural waveguides," *The Journal of the Acoustical Society of America* **117**, 2835.

- Mahapatra, D., Singhal, A., and Gopalakrishnan, S., 2006, "A higher-order finite waveguide model for spectral analysis of composite structures," *Computer Methods in Applied Mechanics and Engineering* **195(9&12)**, 1116–1135.
- Nayfeh, A., 1991, "The general problem of elastic wave propagation in multilayered anisotropic media," *The Journal of the Acoustical Society of America* **89**, 1521.
- Roy Mahapatra, D. and Gopalakrishnan, S., 2003, "A spectral finite element model for analysis of axial–flexural–shear coupled wave propagation in laminated composite beams," *Composite Structures* **59(1)**, 67–88.
- Shorter, P., 2004, "Wave propagation and damping in linear viscoelastic laminates," *The Journal of the Acoustical Society of America* **115**, 1917.
- Timoshenko, S. and Goodier, J., 1970, *Theory of Elasticity [M]*, MacGraw Hill, New York, pp. 328–333.
- Żak, A., Krawczuk, M., and Ostachowicz, W., 2006, "Propagation of in-plane elastic waves in a composite panel," *Finite Elements in Analysis and Design* **43(2)**, 145–154.